Supplementary Information section

In vivo target occupancy by bivalent- and induced-fit type binding drugs

Running title: PK-PD modelling of 2-step binding drugs.

Georges Vauquelin

Department Molecular and Biochemical Pharmacology, Vrije Universiteit Brussel, Pleinlaan 2, B-1050 Brussels, Belgium.

Table of Contents **Page**

(Table S1) Binding constants and parameters for an extended range of 2-step binding drugs.

The difference in Gibbs free energy between the ground state R and the final R'L state is kept constant for all ligands and their $(k_2.k_4)/(k_1.k_3)$ ratio is arbitrarily set to $4x10^{-9}$ M such as in Vauquelin et al. (2016a). k_1 Is also kept constant at 1.10^6 $M^{-1}min^{-1}$. The binding properties are then only controlled by k_2 and k_3. The "grid" on top represents a two-dimensional "kinetic space" that shows the investigated k_2 - k_3 combinations. Data in Table S1 apply to all the cases of the grid and data shown in Figures S2 and S4 apply to the drugs that are assigned by the highlighted cases, or to part thereof, such as indicated.

The orange diagonal line in the grid separates the drugs into two distinct categories. Those above (with the "bivalent" like binding Drug A as prototype) are characterized by $k_2 < k_3$ (which implies that RL converts preferentially into R'L than to dissociate) so that $k_1.K_D$* constitutes the upper limit for k_{off}. Those below (with the "induced-fit"like binding Drug B as prototype) are characterized by $k_2 > k_3$ (which implies that RL dissociates preferentially) so that k_4 now constitutes the upper limit for k_{off}.. The drugs that are situated on the diagonal line are characterized by $k_2 = k_3 + k_4$ (or $\approx k_3$ since k_4 is 5- to 1000-fold less than k_3 for all the presently investigated drugs). Comparing the data in Sections C and D of Table S1 reveals that the so-calculated Diss $t_{1/2}$ is in excellent agreement with those that are based on simulated *in vitro* washout experiments.

Sections A to E of Table S1 provide the following parameters for all the drugs shown in the grid: (values for Drug A and B are highlighted in red):

A) The microscopic rate constant k_4 equals $(K_D.k_1.k_3)/k_2$.

B) The "macroscopic"/pseudo affinity constant, K_D* (in nM) can be calculated by using Equation 5 in Figure 1B of the article. This parameter corresponds to the concentration of free ligand, [L], at which the occupancy of the target (in where both RL and R'L participates) is half maximal at equilibrium.

C) Diss $t_{1/2}$ (in min) refers to the dissociation half-life (= $0.69/k_{off}$ and closely related to its "residence time" = $1/k_{off}$) calculated by use of Equation 4 in Figure 1B of the article.

D) Diss $t_{1/2}$ (in min) is here based on simulated *in vitro* wash-out experiments; i.e. when the targets are first incubated with free drug and then in fresh medium only (here mimicked by setting [L] = 0). The decline in target occupancy during the second phase can adequately

analyzed according to a mono-exponential decay paradigm by use of Graph-Pad Prism 4.0 (GraphPad Software Inc.).
E) Occ $t_{1/2}$ (in min) refers to the half live with which the *in vivo* target occupancy decreases between 1050 and 1440 min after dosing and is calculated such as mentioned above. Target occupancy vs. time profiles of the highlighted drugs in the grid are shown in Figure 2B of the article.

(Figure S2) Effect of changing the microscopic rate constants on the Diss $t_{1/2}$ and the *in vivo* Occ $t_{1/2}$ values for an extended range of drugs.

The impact of a 10-fold increase of k_1 or k_3 or decrease of k_2 or k_4 on the Diss $t_{1/2}$ and Occ $t_{1/2}$ was only shown for Drugs A and B in Figure 3B of the article. Here, we compare this impact for the 9 highlighted drugs. The Diss $t_{1/2}$ and Occ $t_{1/2}$ values of are very similar for all the parent drugs (see Table S1). The Diss $t_{1/2}$ values of each parent drug, "C", is assigned as unitty for the bar graphs to better appreciate the effect of changing the microscopic rate constants 10-fold. The Diss $t_{1/2}$ and Occ $t_{1/2}$ values are increased by about 10-fold for the $-k_{2L}$, $-k_{3H}$ and $-k_{4L}$ variants of Drug A and the other bivalent like binders, less than 2-fold for the $-k_{2L}$, $-k_{3H}$ variants and about 10-fold for the $-k_{4L}$ variant of the induced-fit like Drug B. An intermediary situation is observed for the drugs that are situated on the diagonal line.

(Figure S3) Mechanisms that are accountable for elevated Occ $t_{1/2}$/Diss $t_{1/2}$ ratios.

Figure S3 explores the relationship between the Occ $t_{1/2}$ of the different drugs and their theoretical Diss $t_{1/2}$ (values for the drugs in the grid are provided in Sections C and E of Table S1). Panel A shows that the Occ $t_{1/2}$ values do always exceed the input Diss $t_{1/2}$ values and that a late data collection practice allows this excess to be kept minimal (i.e. < 10 %) for a widest range of drugs.

The Occ $t_{1/2}$/Diss $t_{1/2}$ ratio is higher for drugs that dissociate only moderately slower than their PK-elimination,. This suggests that the elimination of such drugs is still able to endow an additional boost of their Occ $t_{1/2}$ values. As shown in Panel B, the high Occ $t_{1/2}$/Diss $t_{1/2}$ ratio for the relatively fast dissociating Drug A can indeed be ascribed to the remaining presence of free drug during the 1050-1440 min post- dosing interval (i.e. when the data are collected for the calculation of the Occ $t_{1/2}$ values). To this end, the occupancy profile is

simulated till 1050 min post-dosing as usual. Then, the remaining [L] is set to 0 or further eliminated with a $t_{1/2}$ of 30, 60, 120 (in black, i.e. same as the elimination $t_{1/2}$ before) or 240 min. The simulations reveal that the Occ $t_{1/2}$ of Drug A during the remaining 1050-1440 min post-dosing interval equals its Diss $t_{1/2}$ when [L] is set to 0 and increases on par with the substitute elimination $t_{1/2}$ rates.

In agreement with the lower Occ $t_{1/2}$/Diss $t_{1/2}$ ratio for Drug B (Panel A), the impact of remaining free drug thereon is also significantly reduced (Panel B, top right). At the other extreme, this impact is high again for the very slow dissociating B-k_{4L} variant (bottom left). a A late appearance of peak occupancy by this variant is clearly illustrated by similar simulations but in where the PK-elimination rate changes earlier (i.e. at 770 instead of 1050 min after dosing (bottom right). This phenomenon is likely to accentuate the impact of remaining free drug on its Occ $t_{1/2}$/Diss $t_{1/2}$ ratio.

(Figure S4) Relationship between T/P ratio's and Occ $t_{1/2}$ values: effect of rebinding and dosage.

Figure S4 explores the relationship between the T/P ratios and the Diss $t_{1/2}$ values (which can be measured during early stages in drug development) and also with the Occ $t_{1/2}$ values for an extended range of drugs and conditions. Whereas a positive correlation between the T/P ratios and those kinetic parameters seems intuitively logical, it is remarkable that it can already be quite closely be rendered by a mono-exponential paradigm, but a bi-exponential paradigm (used here) is even better.

Panel A refers to a situation without rebinding and depicts the T/P ratios vs. the Diss $t_{1/2}$ values (left side) and vs. the 1050-1440 min- based Occ $t_{1/2}$ values (right side) at day 1 for the 9 highlighted drugs in Table S1 and their variants whose microscopic rate constants differ 3.3 as well as 10-fold. The Occ $t_{1/2}$ values that are gathered after 8 daily dosings (i.e. day 8) are not shown since they are nearly identical to those at day 1. The data (red dots) closely tally with a bi-exponential paradigm (black line with R^2 = 0.993 and Occ $t_{1/2}$ = 0.983, respectively). The T/P ratio is half-maximal at Diss $t_{1/2}$ = 850 min and for Occ $t_{1/2}$ = 928 min. This close fit stems from the relatively modest difference between the Diss $t_{1/2}$- and Occ $t_{1/2}$ values of each drug (See Table S1 and Figure S3).

Panel B depicts the relationship between the T/P ratio and the Occ $t_{1/2}$ values (red dots) that are gathered in the presence of rebinding at day 1 (left side) and day 8 (right side) for the same drugs as in Panel A. The relationship between both parameters at day 1 as well as at day 8 can here also be recounted by a bi-exponential paradigm (black line with R^2 = 0.987 and 0.992, respectively). The T/P ratio is half-maximal at Occ $t_{1/2}$ = 899 and 1013 min, respectively. Those parameters compare well with those recorded in the absence of rebinding (Panel A). Hence, rebinding does not substantially affect the relationship between the T/P ratios and the Occ $t_{1/2}$ values.

Panel C refers to a situation without rebinding and depicts the T/P ratios vs. the Diss $t_{1/2}$ values (left side) and vs. the 1050-1440 min- based Occ $t_{1/2}$ values (right side) at day 1 for a 10-fold higher dosage (i.e. $[L_{max}]/K^*_D$ = 90 instead of 9) for Drugs A, B and an intermediary drug (with $k_2 = k_3 = 4$ min^{-1}, see Table S1) and their variants such as in Panel A. Here again, these relationships can be recounted by a bi-exponential paradigm (black line with R^2 = 0.999 and 0.998, respectively). The T/P ratio is half-maximal for Diss $t_{1/2}$ = 554 min and for Occ $t_{1/2}$ = 734 min. The presently quite low Diss $t_{1/2}$ value may be related to the only late decline in target occupancy at this high dosage (such as shown in Figure 5C of the article). The data that are gathered at day 8 are not shown since they are closely similar to those at day 1.

References.

Garret ER (1994) The Bateman function revisited: a critical evaluation of the quantitative expressions to characterize concentrations in the one compartment body model as a function of time with first-order invasion and first-order elimination. *J Pharmacokinet Biopharm* **22**: 103-128.

Vauquelin G, Morsing P, Fierens FLP, De Backer J-P, Vanderheyden PML (2001). A two-state receptor model for the interaction between angiotensin II AT_1 receptors and their non-peptide antagonists. *Biochem Pharmacol* **61**: 277-284.

Table S1

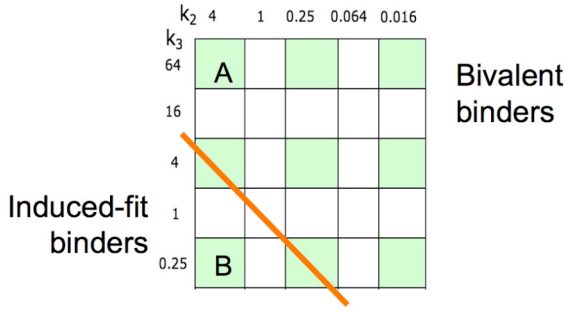

A) k_4 (min^{-1})

$k_3\backslash k_2$ (min^{-1})	4	1	0.25	0.064	0.016
64	0.064	0.25	1	4	16
16	0.016	0.064	0.25	1	4
4	0.004	0.016	0.064	0.25	1
1	0.001	0.004	0.016	0.064	0.25
0.25	$2.5.10^{-4}$	0.001	0.004	0.016	0.064

B) K_D* (nM)

$k_3\backslash k_2$ (min^{-1})	4	1	0.25	0.064	0.016
64	4.00	3.89	3.85	3.76	3.20
16	4.00	3.98	3.85	3.76	3.20
4	4.00	3.98	3.94	3.76	3.20
1	4.00	3.98	3.94	3.85	3.20
0.25	4.00	3.98	3.94	3.85	3.26

C) Diss $t_{1/2}$ in min (= $0.69/k_{off}$, via equation 4 in Figure 1B of the article)

$k_3\backslash k_2$ (min^{-1})	4	1	0.25	0.064	0.016
64	183	180	180	183	216
16	216	184	182	184	216
4	345	216	186	186	216
1	863	346	218	190	218
0.25	2933	863	348	222	222

D) Diss $t_{1/2}$ in min (from simulated washout experiments)

$k_3\backslash k_2$ (min^{-1})	4	1	0.25	0.064	0.016
64	184	177	177	184	217
16	217	185	179	185	217
4	346	217	187	187	217
1	870	345	219	195	219
0.25	2983	818	341	225	225

E) Occ $t_{1/2}$ in min (for the 1050-1440 min interval after dosing)

$k_3\backslash k_2$ (min^{-1})	4	1	0.25	0.064	0.016
64	230	224	222	230	261
16	259	230	226	230	259
4	381	259	232	232	261
1	898	381	260	239	260
0.25	3090	899	382	267	264

Figure S2

Diss $t_{1/2}$ and Occ $t_{1/2}$ values of an extended range of drug variants

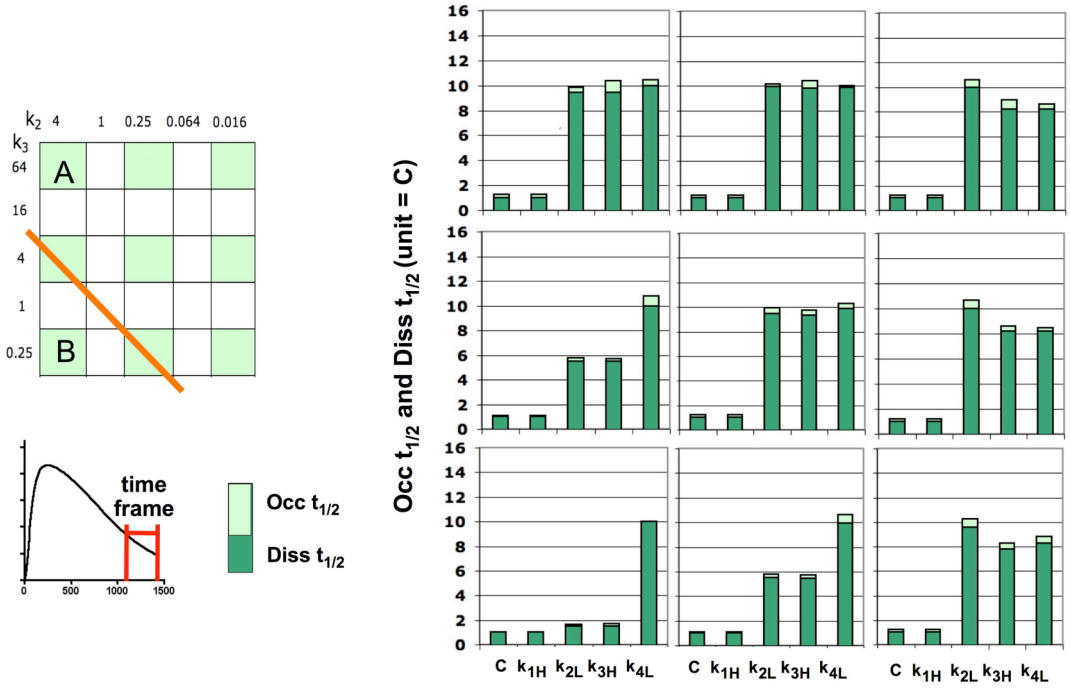

Figure S3

A) Difference between Occ $t_{1/2}$ and Diss $t_{1/2}$

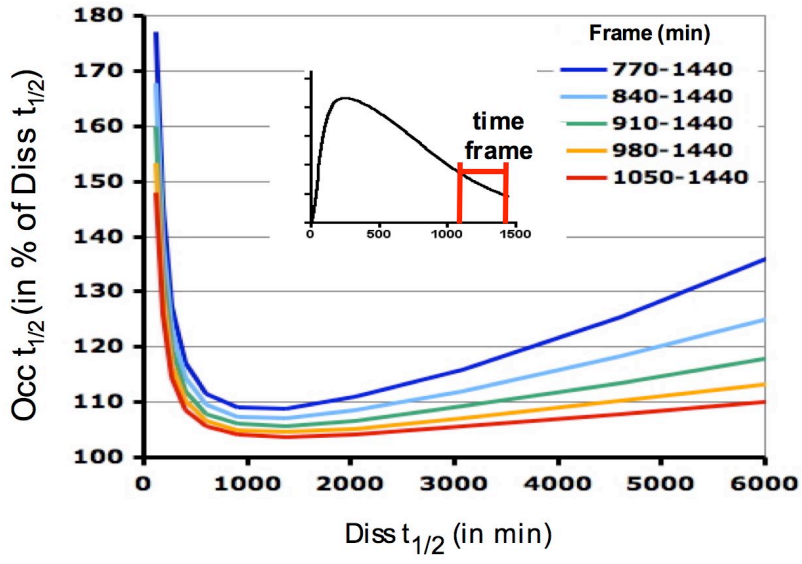

B) Occupancy profiles

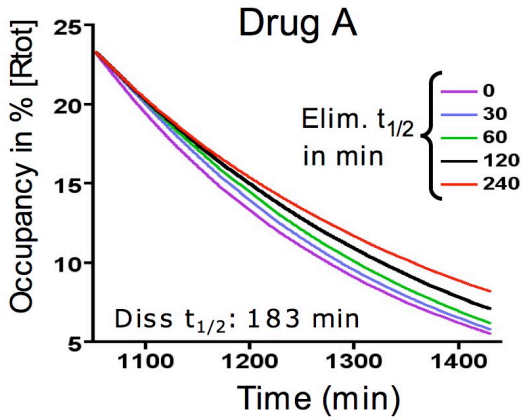

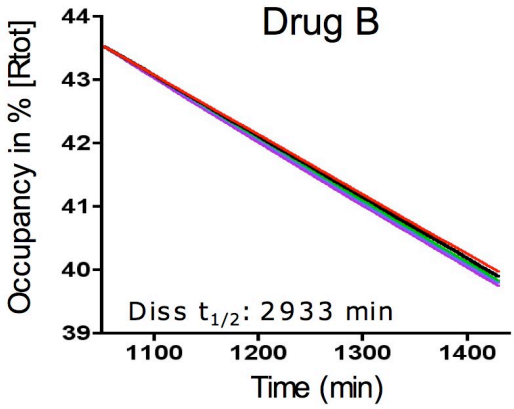

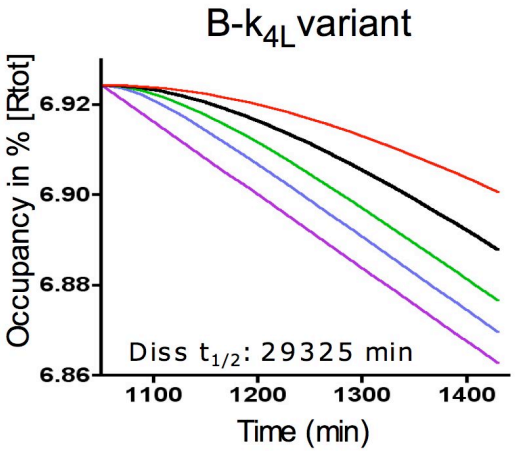

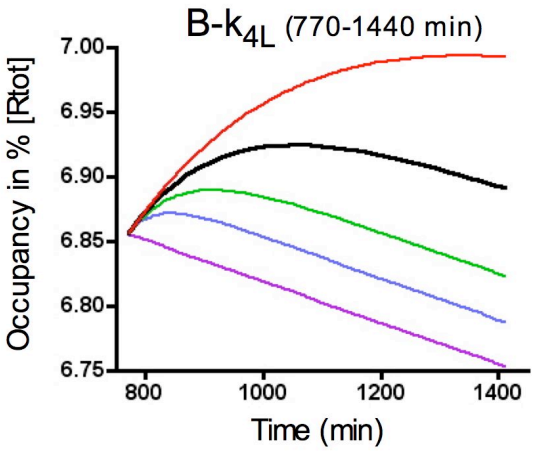

Figure S4

A) T/P ratio vs Diss $t_{1/2}$ and Occ $t_{1/2}$ values without rebinding

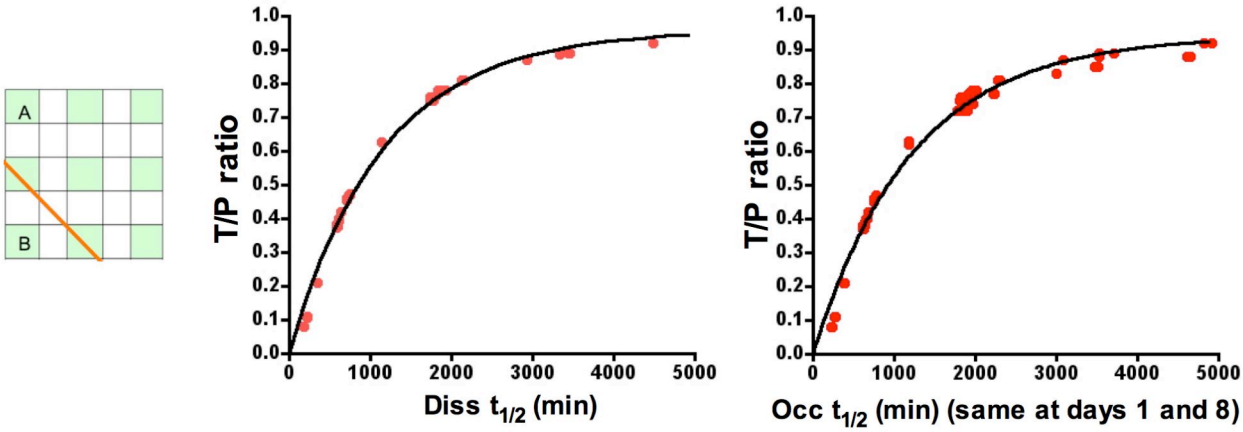

B) T/P ratio vs Occ $t_{1/2}$ values at days 1 and 8 in presence of rebinding

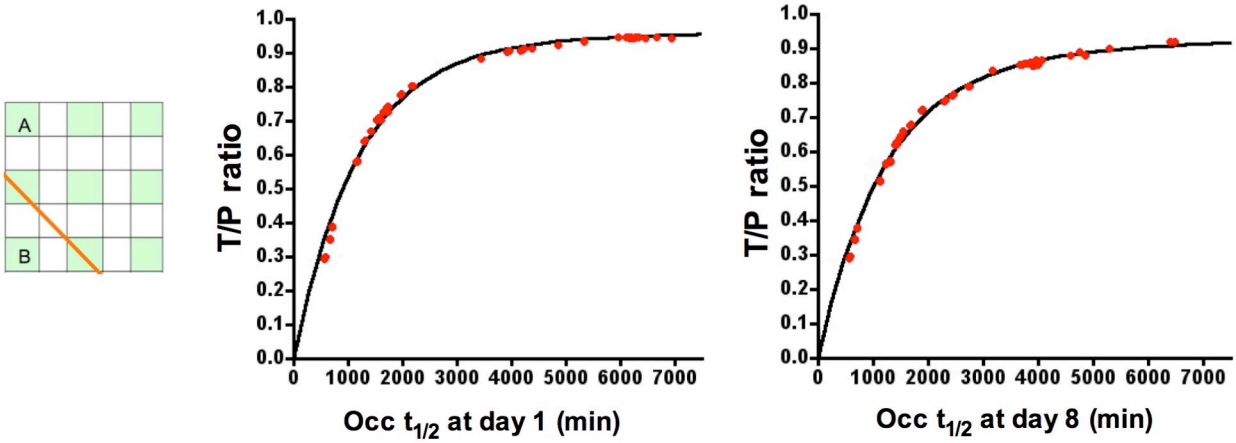

C) T/P ratio vs Diss $t_{1/2}$ and Occ $t_{1/2}$ values at a 10-fold higher dosage